Proc. Natl. Acad. Sci. USA
Vol. 93, pp. 7460–7463, July 1996
Applied Biological Sciences

In vivo tissue distribution of CD4 lymphocytes in mice determined by radioimmunoscintigraphy with an ^{111}In-labeled anti-CD4 monoclonal antibody

ROBERT H. RUBIN*†, DAVID BALTIMORE‡, BENJAMIN K. CHEN§, ROBERT A. WILKINSON†, AND ALAN J. FISCHMAN*†

*Center for Experimental Pharmacology and Therapeutics, Harvard University–Massachusetts Institute of Technology Division of Health Sciences and Technology, Cambridge, MA 02139; †Division of Nuclear Medicine, Department of Radiology, Massachusetts General Hospital and Harvard Medical School, Boston, MA 02114; ‡Department of Biology, Massachusetts Institute of Technology, Cambridge, MA 02139; and The Rockefeller University, New York, NY 10021

Contributed by David Baltimore, April 7, 1996

ABSTRACT **The tissue distribution of CD4 lymphocytes in normal C57/BL mice and CD4 knockout mice was determined by biodistribution measurements and gamma camera imaging with an ^{111}In- labeled rat IgG_{2b} monoclonal antibody directed against the murine CD-4 antigen. In normal mice, high concentrations of antibody accumulated in the spleen and lymph nodes. At 45 hr after injection, the concentrations of radiolabel in the spleen and lymph nodes of normal mice were 10- to 20-fold greater than in the corresponding tissues of the CD4 knockout mice and nonlymphoid tissues of both types of mice. At 24 and 45 hr, gamma camera images showed high concentrations of radiolabeled antibody in lymph nodes and spleen of normal but not knockout mice. These results indicate that radioimmunoscintigraphy with ^{111}In-anti-CD4 is an excellent method for studying tissue distribution of CD4 lymphocytes in mice. Using an equivalent anti-human CD4 antibody, this method might be useful for studying the pathophysiology of conditions in which these cells play a critical role and for monitoring therapies for these disorders.**

From the early days of the human immunodeficiency virus (HIV) epidemic, it has been apparent that the CD4-positive lymphocyte is the major target of this virus (1). Although HIV is capable of infecting other cells such as monocytes (2–4), follicular dendritic cells (5), epidermal Langerhans cells (6), alveolar macrophages (7), and glial cells within the central nervous system (8–10), the CD4-positive lymphocytes bear the brunt of viral attack. Thus, enumeration of CD4 cells in the peripheral blood has been the most widely used test for monitoring HIV-induced immune dysfunction, as well as serving as a surrogate marker for evaluating anti-viral drug efficacy (11).

Unfortunately, this simple test, the "peripheral CD4 count," has not proven as useful for these purposes as had been originally hoped. It is now recognized that major functional alterations in immunity may be unrecognized by CD4 cell enumeration alone: (*i*) there is considerable day-to-day variability in CD4 counts within a given individual; (*ii*) CD4 counts do not provide any information about lymphocyte function; (*iii*) the peripheral blood compartment comprises only 2–5% of the total body lymphoid tissue, and important changes in CD4 cell trafficking and distribution may not be represented by measurements that sample only the peripheral blood compartment; and (*iv*) most importantly, serial determination of CD4 levels as a marker for anti-viral efficacy has proven to be a disappointment—i.e., maintenance or elevations in CD4 cell counts achieved in association with antiviral therapy have not been predictive of prolonged life or decreased incidence of opportunistic infection (1, 11, 12).

The publication costs of this article were defrayed in part by page charge payment. This article must therefore be hereby marked "*advertisement*" in accordance with 18 U.S.C. §1734 solely to indicate this fact.

Thus, there remains a compelling need for a noninvasive test for assessing the totality of CD4 cell distribution and trafficking throughout the body. Such a technique would be invaluable both for evaluating individual patients with HIV infection and as an experimental tool in the assessment of candidate therapies for this disease. In addition, it would be of interest in the evaluation of patients with such autoimmune processes as rheumatoid arthritis and multiple sclerosis, in whom immunomodulating therapy has much to offer. We report here the initial evaluation, in a murine model, of the use of a specific radiolabeled anti-CD4 mAb and serial gamma camera imaging to delineate the tissue distribution of CD4-positive lymphocytes.

MATERIALS AND METHODS

Preparation of ^{111}In-Labeled Antibody. GK1.5, a rat IgG_{2b} noncytotoxic mAb directed against the murine CD-4 antigen (13), was graciously provided as crude ascites by Hugh Auchincloss (Transplant Unit, Massachusetts General Hospital). Rat IgG was isolated from the ascites by a two-step method of ammonium sulfate precipitation, followed by protein G purification, as described (14). HPLC analysis of the resulting protein solution using a size exclusion column revealed a single protein peak that eluted with a retention time corresponding to monomeric IgG.

This antibody was conjugated with diethylenetriamine pentaacetic acid (DTPA) by the carboxy-carbonic anhydride method (15, 16). The DTPA-antibody conjugate was diluted to 2 mg of protein per millimeter (in 0.9% sodium chloride for injection; U.S. Pharmacopeia) and sterilized by membrane filtration. Aliquots of 0.1 ml were transferred aseptically to 2-ml sterile and pyrogen-free vials and stored at 4°C for subsequent labeling with ^{111}In.

The DTPA-antibody conjugate was radiolabeled with sterile, pyrogen-free ^{111}In chloride as follows: GK1.5–DTPA (50 μl, 100 μg) was mixed with 50 μl of 1 N sodium citrate (pH 5.3) and 5 μl (≈3 mCi; 1 Ci = 37 GBq) of ^{111}In chloride (NEZ 304, DuPont/NEN) was added, The solution was incubated at room temperature for 4 hr and the radiolabeled protein was separated on a 1 × 30 cm size-exclusion column (Sephadex G-25–80) eluted with 0.9% sodium chloride.

CD4 Binding Assay. DTPA-conjugated GK1.5 was tested *in vitro* to confirm that it had not lost its ability to bind with high specificity to CD4 expressed on murine splenocytes. Splenocytes harvested from C57/BL mice were incubated with DTPA–GK1.5 (5 μg/ml) or a control isotype matched antibody directed against murine CD4 (clone YTS 191.1). The splenocyte–antibody complexes were then incubated with anti-Rat IgG_{2b} antibody conjugated with fluorescein isothiocyanate (PharMingen) and analyzed by fluorescence activated flow cytometry (FACScan, Becton Dickinson).

Flow cytometric analysis indicated that an equivalent number of CD4 cells, as a fraction of total splenocytes, could be detected with both DTPA–GK1.5 and the unmodified anti-

body. Furthermore, when bound to CD4+ splenocytes, DT-PA–GK1.5 was detected by anti-Rat IgG_{2b}-fluorescein isothiocyanate with equal or greater fluorescence intensity compared with the unmodified antibody.

Imaging and Biodistribution Studies. Groups of normal C57/BL and CD-4 knockout mice weighing ≈25 g (The Jackson Laboratory) were used in these studies. All radiopharmaceuticals were injected intravenously via the tail vein and biodistribution/gamma camera imaging were performed as described below.

Effect of Specific Activity of ^{111}In-Labeled GK1.5 on Biodistribution and Gamma Camera Imaging. Six normal C57/BL mice were injected with 10 μCi of ^{111}In-labeled GK1.5 containing 0.4, 9.7, or 99.7 μg of unlabeled antibody protein. At 24 hr post-injection the animals were sacrificed by anesthesia overdose, and the organs removed for biodistribution studies. Samples of blood, liver, spleen, thymus, mesentery, kidney, bone, and lymph nodes were weighed and radioactivity was measured with a well-type gamma counter (LBK model 1282 Wallae Oy, Finland). To correct for radioactive decay, aliquots of the injected doses were counted simultaneously. The results were expressed as percentage injected dose per gram (% ID/g).

Three additional normal C57/BL mice were injected with 100 μCi of ^{111}In-labeled GK1.5 containing 13, 22, or 112 μg of unlabeled antibody protein. At 24 hr post-injection the animals were anesthetized with ether and whole body scintigrams were acquired using a large field of view gamma camera equipped with a pin-hole collimator containing a 3-mm insert and interfaced to a dedicated computer system (Technicare 410/Technicare 560, Solon, OH). Images were recorded for a preset time of 5 min per view with windows centered on the 174 and 247 KeV photopeaks of ^{111}In.

Effect of CD4 Gene Expression on Imaging and Biodistribution. Normal C57/BL and CD-4 knockout mice (n = 6/group) were injected with 100 μCi of ^{111}In-labeled GK1.5 containing 5.4 μg of protein, and gamma camera imaging/biodistribution measurements were performed as described above. In this study, the animals were imaged at 2.5, 24, and 45 hr after injection. In one additional normal mouse imaging was performed 60 hr after injection.

Statistical Methods. The results of all experiments were evaluated by analysis of variance using a linear model in which tissue and antibody dose or CD4 status (normal C57/BL or CD4 knockout) were the classification variables (% ID/g = tissue + antibody dose + tissue * antibody dose or %ID/g = tissue + CD4 status + tissue * CD4 status). Post hoc comparisons of individual means were performed by Duncan's new multiple range test (17). All results were expressed as mean ± SEM.

RESULTS

To examine whether a radiolabeled anti-CD4 antibody will home to antigen-containing cells in an animal's body, we injected 100 μCi of ^{111}In-labeled GK1.5 mAb into normal mice. Serial gamma camera images were acquired 2.5, 24, 45, and 60 hr later (Fig. 1). The earliest image showed significant concentration of radioactivity in the blood pool, diffuse distribution of radioactivity throughout the rest of the body, and low levels of focal accumulation in axillary and inguinal lymph nodes and spleen. In the 24-hr image, clear focal accumulation of radiolabeled antibody was observed in cervical, axillary, and inguinal lymph nodes and spleen. This focal accumulation intensified in the 45-hr image and remained unchanged to 60 hr. Gamma camera images were then acquired 24 hr after injection of radiolabeled antibody at three different specific activities (Fig. 2). The highest specific activity antibody gave clear focal accumulation of radioactivity in the spleen and lymph nodes. In the intermediate specific activity image, the focal localization of radioactivity was significantly reduced,

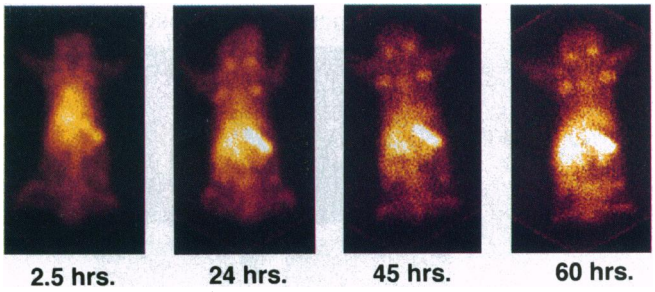

FIG. 1. Serial gamma camera images of a normal mouse acquired 2.5, 24, 45, and 60 hr after injection of 100 μCi of ^{111}In-labeled GK1.5 anti-CD4 mAb.

and it was totally abolished in the low specific activity image. Thus, competitive inhibition of the localization of labeled antibody by increasing concentrations of unlabeled antibody was evident.

To determine whether the focal accumulations of radioactivity were due to binding of antibody to surface CD4 on cells, we compared images acquired from normal and $CD4^{-/-}$ mice (Fig. 3). At 24 and 45 hr after injection there was a highly localized antibody in the lymph nodes and spleen of the normal animals that was not evident in the knockout mice.

Having seen the focal accumulations visually we turned to biodistribution measurements to examine the binding more quantitatively. These were performed 24 hr after injection of the ^{111}In-labeled anti-CD4 mAb into normal mice and demonstrated particularly high concentrations of antibody associated radioactivity in the spleen and lymph nodes. When increasing quantities of unlabeled antibody were added to a fixed amount of radiolabeled antibody (thus decreasing specific activity) there was a dose-dependent decrease in the amount of radiolabeled antibody that localized in the spleen (Fig. 4). In the other tissues, however, the results were variable, suggesting that the CD4 may not be saturated by these amounts of antibody.

When studies were performed 45 hr after the injection of the radiolabeled mAb in normal and CD4 knockout mice, a striking difference in biodistribution was observed (Fig. 5). In the normal mice, the concentrations of radiolabel in the spleen and lymph nodes was 10- to 20-fold greater than in the corresponding tissues of the CD4 knockout mice ($P < 0.0001$) and 10- to 20-fold greater than the concentrations achieved in nonlymphoid tissues of both normal and CD4 knockout mice ($P < 0.0001$). Similar but smaller effects were observed in mesentery ($P < 0.01$) and bone ($P < 0.05$). In contrast, higher concentrations of antibody were observed in blood of CD4 knockout mice ($P < 0.01$). In liver and thymus, antibody accumulation was similar in normal and CD4 knockout mice (P = not significant).

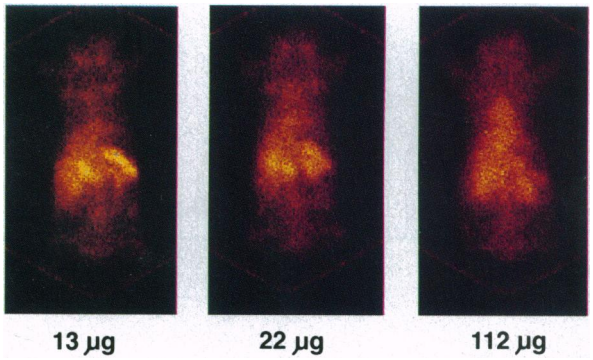

FIG. 2. Gamma camera images demonstrating the effect of specific activity of ^{111}In-labeled GK1.5 anti-CD4 mAb on localization in spleen and lymph nodes.

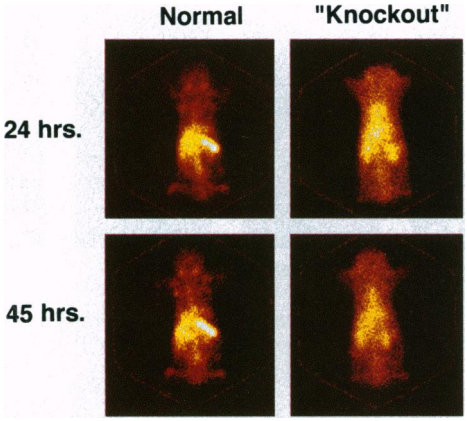

FIG. 3. Serial gamma camera images acquired 24 and 45 hr after injection of ^{111}In-labeled GK1.5 anti-CD4 mAb in normal C57/BL mice and syngenetic CD4 knockout mice.

These two biodistribution studies suggest that the localization of the radiolabeled CD4 antibody in lymphoid tissue of the mouse is mediated by specific, rather than nonspecific, mechanisms. Furthermore, the differences in tissue accumulation of radiolabeled antibody were clearly sufficient to permit noninvasive imaging of the distribution of this antibody.

DISCUSSION

These experiments were designed to evaluate the feasibility of using a radiolabled mAb to measure the tissue distribution and, potentially, the trafficking of CD4-positive lymphocytes. The results suggest that specific localization of the radiolabeled antibody occurs in the spleen and lymph nodes. Specificity is shown by two sets of experiments: (*i*) blockade of specific localization by increasing doses of unlabeled antibody that is consistent with competition for a limited number of specific antigenic sites and (*ii*) failure of localization of the radiolabeled antibody to lymphoid tissue in CD4 knockout mice. In addition, a nonspecific mAb labeled with indium-111 in identical fashion failed to image the spleen and lymph nodes (18). The effect of an increasing dose of unlabeled antibody on localization of ^{111}In–GK1.5 was observed in both the biodistribution and imaging experiments. However, the degree of blockade was greater in the biodistribution studies. This was probably due to the relatively low specific activity of the product of radiolabeling and the requirement of larger amounts of radioactivity for imaging. Due to these constraints, even the highest specific activity preparation used in the

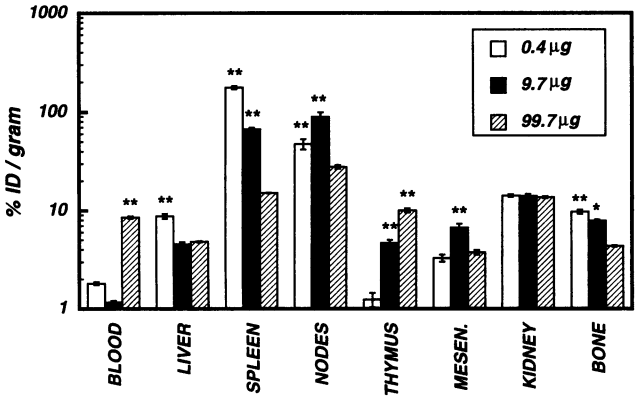

FIG. 4. Effect of specific activity on the biodistribution of ^{111}In-labeled GK1.5 anti-CD4 mAb in normal C57/BL mice 24 hr after injection. Each value is the mean ± SEM for six animals. **, $P < 0.01$; *, $P < 0.05$.

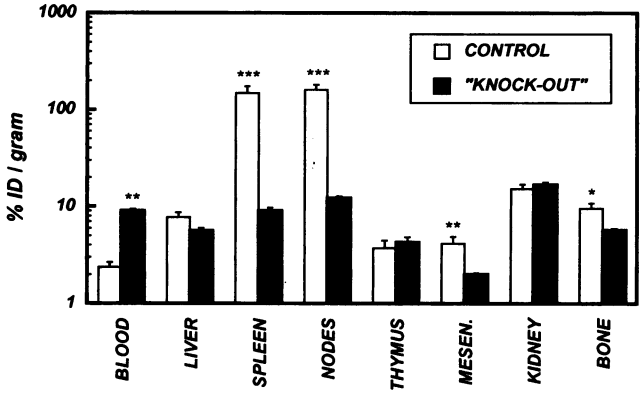

FIG. 5. Biodistribution of ^{111}In-labeled GK1.5 anti-CD4 mAb (5.7 μg/100 μCi) in normal C57/BL mice and syngenetic CD4 knockout mice 45 hr after injection. Each value is the mean ± SEM for six animals. ***, $P < 0.001$; **, $P < 0.01$; *, $P < 0.05$.

imaging studies (13 μg per mouse; Fig. 2) contained a mass of unlabeled antibody sufficient to produce considerable blockade. Although the effect of an increasing amount of unlabeled antibody in the injected dose resulted in a monotonic reduction in accumulation of radioactivity in the spleen, a biphasic effect was observed in the lymph nodes. This could be related to differences in the concentration of antigenic sites in the two tissues and mass-action considerations.

The observation that the specific localization that occurs is of an extent sufficient to permit imaging is important, because it provides a noninvasive approach for evaluating serially the distribution of CD4-positive lymphocytes during the course of disease or its therapy. Thus, experimentally, this approach might be useful for studying murine models of autoimmune disease such as allergic encephalomyelitis, collagen induced arthritis, and the spontaneously occurring lupus-like syndromes of NZB/NZW mice, as well as candidate therapies for these conditions.

Clearly, the more important implication of these results is the potential application of the approach to the study of humans. There is considerable precedent for studying the trafficking in leukocyte populations *in vivo* in humans by nuclear medicine techniques. In particular, the migration of polymorphonuclear leukocytes from peripheral blood to sites of focal infection has been applied as a diagnostic test and two different approaches have shown clinical utility. With the first method, blood is drawn from the individual, polymorphonuclear leukocytes are isolated and radiolabeled with either ^{111}In or ^{99m}Tc, and the labeled cells are re-infused (19–21). In the second method, a mAb specific for a polymorphonuclear leukocyte cell surface antigen is radiolabeled with either ^{111}In or ^{99m}Tc, and infused into the subject, with subsequent *in vivo* labeling of circulating and tissue bound polymorphonuclear leukocytes (22, 23). With both techniques, the radiolabeled cells are followed by serial gamma camera imaging (typically over 12–48 hr post-infusion), to detect focal accumulation at the site of infection (19–23).

The imaging and biodistribution studies reported here further extend this approach. Our results indicate that a specific, high-affinity mAb directed against a lymphocyte cell surface marker can be used for *in vivo* studies of the tissue distribution and trafficking of particular lymphocyte subpopulations—in this case CD4-positive lymphocytes. In addition to the semiquantitative nature of the imaging data that is obtained, the noninvasive character of this approach provides an opportunity for serial studies to assess disease progression and the response to therapy. The application of this technique for the serial study of HIV infection and a variety of autoimmune conditions in humans is obvious. Since only tracer amounts of antibody are required for imaging, these studies should not produce significant perturbations of the immune system.

1. Schooley, R. T. (1994) in *Clinical Approach to Infection in the Compromised Host*, eds. Rubin, R. H. & Young, L. S. (Plenum, New York), 3rd Ed., pp. 411–422.
2. McElrath, M. J., Pruett, J. E. & Cohn, Z. A. (1989) *Proc. Natl. Acad. Sci. USA* **86,** 675–679.
3. Ho, D. D., Rota, T. R. & Hirsch, M. S. (1986) *J. Clin. Invest.* **77,** 1712–1715.
4. Popovic, M. & Gartner, S. (1987) *Lancet* **ii,** 916.
5. Tenner-Racz, K., Racz, P., Dietrich, M. & Kern, P. (1985) *Lancet* **i,** 1105–1106.
6. Tschachler, E., Groh, V., Popovic, M., Mann, D. L., Konrad, K., Safai, B., Eron, L., diMarzo, V. F., Wolff, K. & Stingl, G. (1987) *J. Invest. Dermatol.* **88,** 233–237.
7. Salahuddin, S. Z., Rose, R. M., Groopman, J. E., Markham, P. D. & Gallo, R. C. (1986) *Blood* **68,** 281–284.
8. Chiodi, F., Fuerstenberg, S., Gidlund, M., Asjo, B. & Fenyo, E. M. (1987) *J. Virol.* **61,** 1244–1247.
9. Koyangi, Y., Miles, S., Mitsuyasu, R. T., Merrill, J. E., Vinters, H. V. & Chen, I. S. (1987) *Science* **236,** 819–822.
10. Cheng-Mayer, C., Rutka, J. T., Rosenblum, M. L., McHugh, T., Stites, D. P. & Levy, J. A. (1987) *Proc. Natl. Acad. Sci. USA* **84,** 3526–3530.
11. Choi, S., Lagakos, S. W., Schooley, R. T. & Volberding, P. A. (1993) *Ann. Intern. Med.* **118,** 674–680.
12. Concorde Coorinating Committee (1994) *Lancet* **343,** 871–881.
13. Dialynas, D. P., Quan, Z. S., Wall, K. A., Pierres, A., Quintans, J., Loken, M. R., Pierres, M. & Fitch, F. W. (1983) *J. Immunol.* **131,** 2445–2451.
14. Harlow, E. & Lane, E. (1988) *Antibodies: A Laboratory Manual* (Cold Spring Harbor Lab. Press, Plainview, NY), pp. 283–318.
15. Krejcarek, G. E. & Tucker, K. L. (1977) *Biochem. Biophys. Res. Commun.* **77,** 581–585.
16. Khaw, B. A., Mattis, J. A., Melincoff, G., Strauss, H. W., Gold, H. K. & Haber, E. (1984) *Hybridoma* **3,** 11–23.
17. Duncan, D. B. (1955) *Biometrics* **11,** 1–42.
18. Rubin, R. H., Young, L. S., Hansen, W. P., Needleman, M., Wilkinson, R., Nelles, M. J., Callahan, R., Khaw, B-A., Strauss, H. W. (1988) *J. Nucl. Med.* **29,** 651–656.
19. McAfee, J. G. & Thakur, M. L. (1976) *J. Nucl. Med.* **17,** 480–487.
20. Datz, F. L. (1994) *Semin. Nucl. Med.* **24,** 92–109.
21. Peters, A. M. (1994) *Semin. Nucl. Med.* **24,** 110–127.
22. Locher, J. T., Seybold, K., Andres, R. Y., Schubiger, P. A., Mach, J. P. & Buchegger, F., (1986) *Nucl. Med. Commun.* **7,** 659–670.
23. Becker, W., Goldenberg, D. M. & Wolff, F. (1994) *Semin. Nucl. Med.* **24,** 142–153.